Comparison of a Linear Least Squares Algorithm and STAR Modal for a Square Elastic Plate

M. Allen, C. Moloney, J. H. Ginsberg, and A. Ferri
The G. W. Woodruff School of Mechanical Engineering
The Georgia Institute of Technology
Atlanta, GA 30332-0405

ABSTRACT

A general linear least squares method for extracting modal parameters from FRF data is described in a companion paper [**J. H. Ginsberg, M. Allen, A. Ferri, and C. Moloney,** *A General Linear Least Squares Algorithm for Identifying Eigenvalues and Residues*, Proceedings of the 21st IMAC, 2003.]. This paper describes an assessment of the algorithm's performance for FRF data obtained from impulse excitation of a free square plate. Although the plate is covered by a polymer on one side, the coating is not constrained, so damping levels are quite low. Because the plate is square, a number of natural frequencies are repeated. The linear least squares algorithm is applied to frequency bands surrounding each frequency. The identified natural frequencies, modal damping ratios, and modal patterns are compared to values obtained from STAR© Modal using an SDOF option.

1 INTRODUCTION

SDOF techniques for modal identification are inherently approximate, for they ignore the multi-modal nature of linear system response. However, they are generally easy to implement, and can offer quick verification of results obtained by sophisticated methods. SDOF identification can also be quite effective for lightly damped systems, especially for the lower modes. A number of texts, such as Ewins [1], and Maia *et al* [2], offer thorough surveys. The objective of the present work is to test another formulation proposed in a companion paper [3]. This method is termed LLS-SDOF, connoting that it is a linear least squares SDOF procedure. When applied to noise-free frequency response data, it is exact for one-degree-of-freedom systems with arbitrary viscous damping, provided that the system is underdamped. The aforementioned reference also demonstrated that it is equally effective at identifying the equivalent modal damping ratio corresponding to a structural damping model.

The present work tests the LLS-SDOF algorithm using vibratory data obtained from a square plate whose edges are free. Results obtained from this technique are compared to those obtained when a readily available commercial package, STAR© modal, is used in an SDOF mode of operation. The comparison examines the natural frequencies and modal damping ratios for the first thirteen modes, as well as mode shape contour patterns for the first four modes. Because the plate is square, certain natural frequencies correspond to two orthogonal modes. However, the measurements followed a MISO protocol, in which it is not possible to distinguish individual modes corresponding to repeated eigenvalues. These multiple modes are treated as a single mode for both LLS-SDOF and STAR modal, as will be described later.

2 EXPERIMENT

A 762 mm × 762 mm × 6.35 mm aluminum plate was subjected to impact testing. The test conditions simulated free boundary conditions. Bungee cords, attached to two adjacent corners of the plate, held it suspended in air. One face of the plate was covered by a 12.7 mm foam damping layer. The system had previously been used for acoustics experiments, for which the foam layer modified the surface impedance. For vibratory phenomena, the foam layer adds little dissipation to the system because it is not constrained on both sides, but it does have an inertial effect. The exposed face of the plate, opposite the foam layer, was divided into a grid composed of 50.8 mm squares. The intersection points not falling on the plate edges, a total of 196, were used as drive points. Initially, three of the grid points also served as the mounting

locations of PCB accelerometers (model: 353 B16). Figure 1 displays the test specimen and the accelerometer placements.

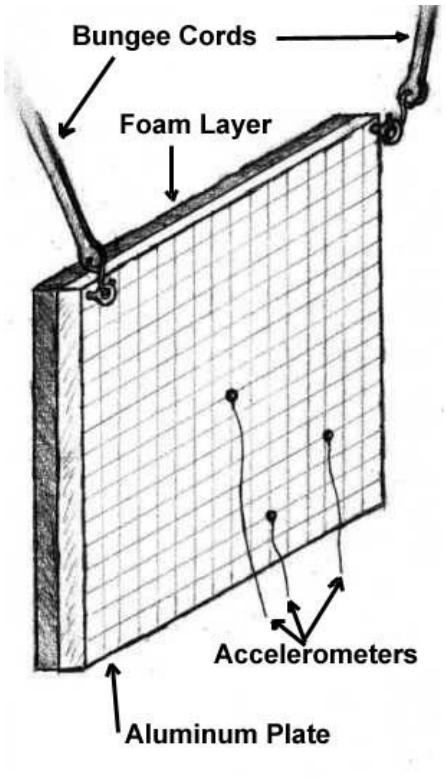

Figure 1: The experimental test specimen - a free square, aluminium plate with unconstrained foam layer.

A PCB modally tuned impact hammer (model: 086 B03) was used to excite the system. A Siglab© data acquisition system, model 20-42, was used to capture the experimental data. The apparatus was set to its maximum resolution of 8192 measurements over a time window of 3.2 sec. Observation of the response to the hammer blows confirmed that this time was adequate for the plate to essentially return to a rest state. These parameters correspond to a time increment of $\Delta t = 39.063$ ms, a frequency increment $\Delta f = 0.3125$ Hz, and a maximum frequency of 1 kHz. The high frequency resolution ensures an adequate number of points will be present around each mode, thus facilitating the curve fitting process during modal parameter extraction. For each impact trial, Siglab recorded the hammer force and accelerometer outputs. Siglab then computed an accelerance transfer function, which was converted in Matlab to a displacement response function (FRF). Only the latter data was stored.

The hammer blows were imparted by hand. All impacts were administered by the same person, and care was taken to keep the hammer head perpendicular to the plate surface. Prior to data collection, several impacts were imparted to check the variability in the procedure. With each strike the FRFs displayed no significant changes, although a detailed error analysis was not performed.

Preliminary measurements were carried out for three accelerometer locations in order to identify which captured the most modes below the 1 kHz limit. This accelerometer was located 203.2 mm to the left and 50.8 mm above the lower right corner of the plate. The data set for the present analysis was obtained from this accelerometer. At each drive point, the system was impacted three times. Siglab averaged the accelerance transfer functions from each impact, resulting in one average FRF for each drive/accelerometer pair. This process was repeated for each of the 196 grid points. The input channels accepting the excitation force and the acceleration responses were set to receive a maximum voltage of 0.63 V. An occasional overload on either the excitation channel or the response channels required that data be discarded and the impact be re-administered.

Figure 2 shows a typical FRF. It will be noted that the frequency in this graph is cutoff at 500 Hz. Beyond that value, the modal density increaseas, making it unlikely that a SDOF approach would yield valid results. Thirteen resonant peaks are visible in the figure. The signal to noise ratio at resonances varies between FRFs. At worst, it was estimated to be 14 dB for a weak low frequency resonance, while the largest maximum signal to noise ratio was estimated to be 35 dB for a strong mid-frequency resonance. Away from resonances, the signal to noise ratio decreases significantly.

3 ANALYSIS PROCEDURES

Curve fitting the frequency response functions (FRFs) captured during experimentation yield the plate's modal parameters: natural frequencies, damping ratios, and residues. STAR Modal's polynomial fit and a the LLS-SDOF algorithm were applied to the same data selected from frequency bands surrounding resonant peaks. The bands could be identified visually in many, but not all, FRFs. For this reason STAR's "Modal Peaks" feature was used to set the frequency bands for all measurement locations. The Modal Peaks feature creates a composite frequency response by accumulating the squared magnitude of each FRF. Each mode then appears as a spike in the composite FRF. A band for each mode was defined by choosing lower and upper frequencies just be-

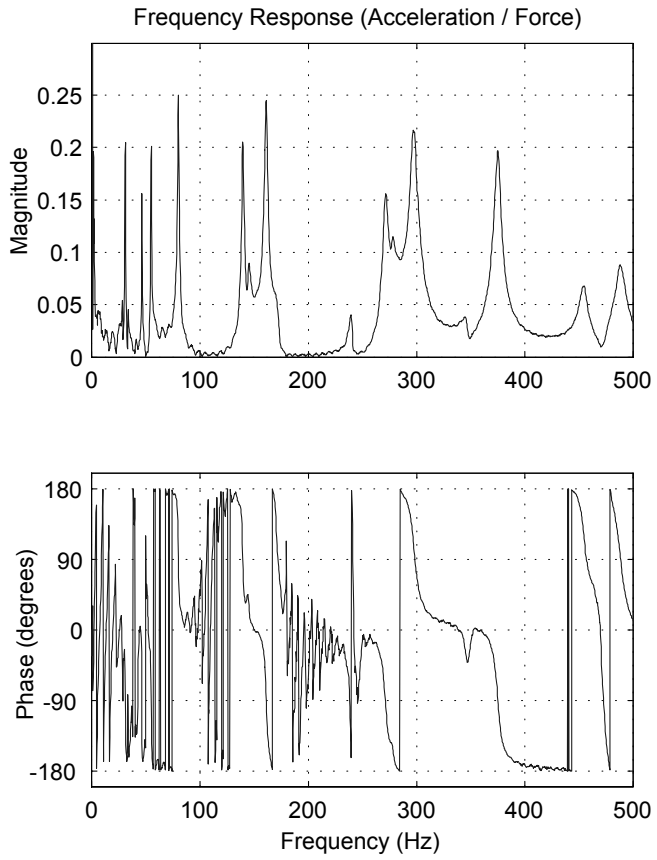

Figure 2: Typical Frequency Response for impulse tests of square plate.

low and above the peak in the composite FRF. Thirteen bands were identified in that operation, capturing all visible modes below 500 Hz.

Each band was assumed to contain only one natural frequency of the system. However, because the plate is square there are a number of frequencies at which a pair of modes exists. In analytical undamped modal analysis the two mode shapes are taken to differ by a 90-degree rotation, leading to a pair that are mutually orthogonal. For experimental work, it is useful to consider the general situation where two modes have close natural frequencies. According to the state-space modal description used by LLS-SDOF and STAR Modal, the contribution of these modes to the FRF between measurement point j and drive point P is given by

$$G_{jP}(s) = \frac{(A_{jP})_1}{i\omega - \lambda_1} + \frac{(A_{jP})_1^*}{i\omega - \lambda_1^*} + \frac{(A_{jP})_2}{i\omega - \lambda_2} + \frac{(A_{jP})_2^*}{i\omega - \lambda_2^*} \quad (1)$$

For a lightly damped system the eigenvalues λ_n and residues A_n are well approximated by undamped modal properties according to

$$\begin{aligned} \lambda_n &= -\zeta_n \omega_n + \left(1 - \zeta_n^2\right)^{1/2} \omega_n i \\ (A_{jP})_n &= \frac{1}{2\omega_n} \Phi_{jn} \Phi_{Pn} \end{aligned} \quad (2)$$

where ω_n is the undamped natural frequency, ζ_n is the modal damping ratio, and Φ_{kn} are the nth set of mode coefficients.

When the two natural frequencies described above merge, there two independent eigenvectors still exist. The only difference between the eigenvalues is their real part, but the small value of ζ_n makes their contributions coalesce. The consequence is that the effective residue becomes $(A_{jP})_1 + (A_{jP})_2$. Analytically, one method for defining orthogonal modes in this situation is to require that the mode shapes when the frequencies are equal closely resemble the shapes when the natural frequencies are slightly different. An alternative is to invoke the Gram-Schmidt orthogonalization procedure, in which one eigenvector is arbitrarily taken as a normal mode. The second normal mode is then as a linear combination of the two eigenvectors, with the coefficient of that combination obtained by enforcing mutual orthogonality. The latter is the viewpoint adopted here. Specifically, the residue factor extracted from the identification algorithm is taken to represent a single mode. Assembling the residues for all measurement points at the same eigenvalue leads to an estimate for the normal mode shape. If one were to repeat the measurements with a different drive point, the resulting residues would lead to a second eigenvector. If that eigenvector is found to differ significantly from the first normal mode, the Gram-Schmidt orthogonalization could be used to determine the second normal mode shape.

3.1 STAR Modal Data analysis with STAR Modal, version 5.22, used the SDOF Polynomial fit technique to estimate the modal parameters. This procedure requires user defined frequency bands, within which an SDOF polynomial model is fit to the data. Contributions of modes outside of the band in focus are ignored, although the fit does include residual terms to account for out-of-band effects. Each of the thirteen frequency bands identified by STAR's Modal Peaks procedure was analyzed in each of the 196 FRF data. Processing this data with STAR modal led to 13 estimated natural frequencies and modal damping ratios that are averages of values obtained from each FRF. Such processing also leads to set of 196 residues (one for each FRF) in each of the 13 frequencies, as well as the corresponding mode coefficients.

3.2 Linear Least Squares A thorough development of the theory behind the LLS-SDOF technique is presented by Ginsberg *et al* [3]. In brief, the LLS-SDOF method begins with the state-space description of a single mode's contribution to an FRF. A series of manipulations leads to sets of linear equations for various combinations of the modal parameter values. When applied to noise-free data representing a viscously damped system, the procedure yields exact values of the natural frequency, critical damping ratio, and residue. Like other SDOF techniques LLS-SDOF assumes that the FRF contribution of modes other than the one in focus are negligible. The fit does not include any residual terms that are intended to correct for out-of-band modes. Noisy data is handled by extending the linear equations to an overdetermined set that are solved in a least-squares sense. The data points for this procedure are selected from bands around each resonant peak. Ginsberg *et al* [3] performed an analysis of the optimal selection of points to minimize the effect of noise, but that analysis was not available when the measurements were made. Instead, all data points falling in the frequency intervals identified by STAR's Modal Peaks procedure were used. Consequently, the same data was used as the input for STAR Modal and for LLS-SDOF. The algorithm was implemented in Matlab.

Another similarity between the analysis using STAR Modal and LLS-SDOF is the manner in which the mode coefficients are computed. Processing each FRF data set with LLS-SDOF yields an estimate for the residue associated with that displacement and each eigenvalue. However, such estimates are not as good as those that are obtained by applying a linear least squares procedure to the full set of FRF data after the eigenvalues have been obtained, see Maia *et al* [2]. The specific details of implementing a linear least squares identification in the context of the present state-space modal formulation were described by Ginsberg, Zaki, and Drexel [4]. STAR Modal proceeds in a similar manner, in that it defers evaluation of the residues and mode coefficients until averaged estimates of the natural frequencies and modal damping ratios have been obtained.

4 RESULTS

The LLS-SDOF algorithm yielded 196 estimates for the natural frequency and damping ratio of each mode, one per FRF data set. The variation of these quantities for the second and fourth modes is displayed in Fig. 3. The data plotted there is the estimated natural frequency and modal damping ratio as a function of the excitation point index of the FRF from which the estimate is derived. The largest excursions of the frequency and damping ratio relative to the average values corresponds to cases where the drive point is close to the mode's node line. At these points the signal to noise ratio for the excitation is very low.

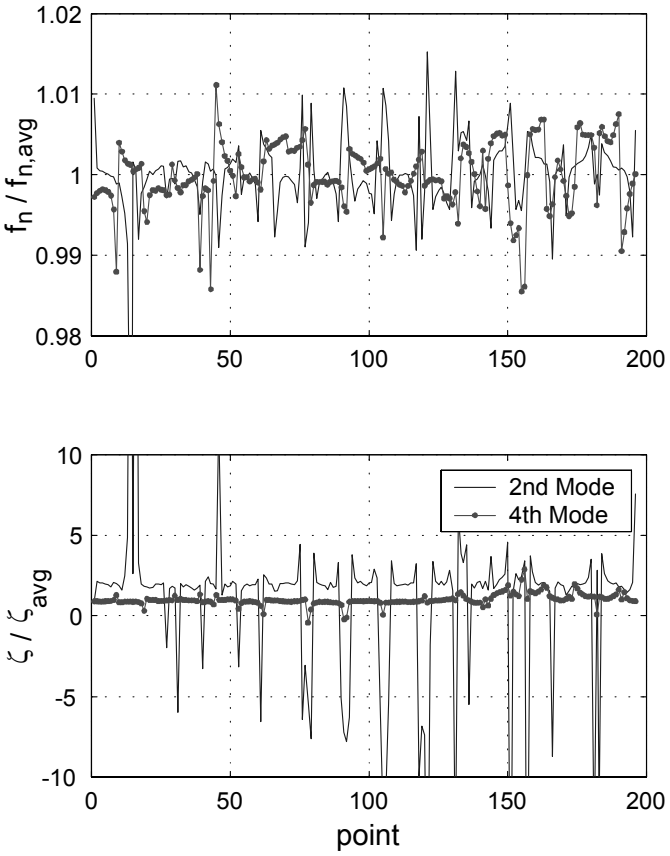

Figure 3: Point to point variation in natural frequency and damping ratio for AMI-SDOF algorithm.

The LLS-SDOF estimates of natural frequency and damping ratio were averaged (using an unweighted average) for comparison with STAR. The documentation for STAR does not indicate if it's averaging is weighted. The results are compared in Table 1. It is noteworthy that the average difference between natural frequencies is 0.5%, with a maximum difference below 1.5%. The damping ratios show much larger differences, especially for the second mode, where STAR Modal output a negative damping ratio. When the second mode is excluded, the average difference between a damping ratio obtained by STAR Modal and LLS-SDOF is 35% of the corresponding mean. Although these differences are larger than one might anticipate, it is usually found that a damping ratio is more difficult to identify than the corresponding natural frequency.

Natural Frequency (Hz)			Damping Ratio*100		
SDOF	STAR	%	SDOF	STAR	%
31.35	31.10	0.79	0.22	0.65	-98.7
46.34	45.80	1.16	0.22	-1.01	-312.1
54.50	54.85	-0.64	0.50	0.61	-20.2
79.93	79.95	-0.02	0.96	0.76	22.8
139.98	140.25	-0.19	0.65	0.46	34.6
161.12	160.56	0.34	1.17	0.80	37.5
169.97	171.21	-0.73	1.96	1.29	41.1
240.10	240.22	-0.05	0.87	0.93	-6.5
273.70	277.78	-1.48	1.01	0.70	36.8
297.40	296.75	0.22	1.43	0.89	46.5
346.88	346.67	0.06	1.14	0.75	40.9
373.66	373.60	0.02	0.90	1.12	-21.3
487.38	488.63	-0.26	1.17	1.30	-10.2

Table 1: Natural frequencies and damping ratios found by LLS-SDOF and STAR Modal algorithm, and the percent difference between the estimates. (Percent difference defined as (LLS-STAR)/mean(LLS,STAR))

As mentioned in the previous section, the normal mode coefficients are obtained with LLS-SDOF after each mode's natural frequency and damping ratio have been estimated. The residues obtained from that estimation process are discarded. Instead, a linear least squares process, based on the eigenvalues being known, was used to compute the residues simultaneously. Doing so reduces estimation error by apprortioning it between all the modes. The computation of the normal mode coefficients corresponding to the residues is described by Ginsberg, Zaki, and Drexel [4]. Details of how STAR Modal extracts the modal coefficients were not provided in the available documentation, but the sequence in which that identification proceeds suggests that the coefficients obtained from STAR Modal also represent a global estimate. The first four mode shapes obtained using LLS-SDOF and STAR Modal are displayed as iso-contours in Figs. 4 to 11. In each graph the modes have been normalized to have unit maximum amplitude. It should be noted that the mode coefficients were found to be essentially real, as one would expect for modes whose damping ratio is below 2%.

The figures indicate that the mode shapes produced by STAR and LLS-SDOF have the same qualitative pattern, though the output of STAR Modal displays a large wavy region near the center for the first two modes. Also, the modal contours derived from STAR modal show more irregularity, which is not what one would expect for low frequency modes. A Nyquist plot of the frequency response data shows that the frequency resolution is somewhat coarse for the first two modes, which may have contributed to the error in these modes.

It should be noted that the fourth mode occurs at the first repeated natural frequency. The corresponding contours shown in Figs. 10 and 11 are valid modes for the system, as noted in the previous discussion of modes having repeated eigenvalues. These modal patterns can also be thought of as a linear combination of two modes: $(a_1 M_1 + a_2 M_2)$, where M_1 is a mode with one horizontal and two vertical node lines, M_2 is the same mode rotated by 90^o, and $a_1 = a_2$, (see Leissa [5] for details). A second MISO experiment (*i.e.* response data obtained when an accelerometer is mounted at a different location) could be used to determine a second linearly independent mode. The two modes would span the same space spanned by M_1 and M_2.

5 CONCLUSIONS

Comparison of modal properties between STAR Modal and a linear least squares SDOF algorithm shows good qualitative agreement. A primary discrepancy was found in the second mode, which STAR Modal indicated to have negative damping. Otherwise, the natural frequencies agreed very well (within 0.5%), while the modal damping ratios showed greater error (35% average error excluding the mode that STAR Modal identified as being negatively damped). The mode shapes determined by the two methods showed the same qualitative pattern. However, some modes obtained from STAR Modal showed small scale irregularities in their contours. This is counter to the expectation that low frequency modes should have reasonably smooth contours.

REFERENCES

[1] **Ewins, D. J**., *Modal Testing: Theory, Practice and Applications,* Second Edition, Research Studies Press Ltd., Baldock, Hertfordshire, England, 2001.

[2] **Maia, S., Silva, J. M. M., He, J., Lieven, N. A. J., Lin, R. M., Skingle, G. W., To, W. M., Urgueira, A. P. V.**, *Theoretical and Experimental Modal Analysis,* Research Studies Press Ltd., Taunto, Somerset, England, 226-227, 1997.

[3] **J. H. Ginsberg, M. Allen, A. Ferri, and C. Moloney,** *A General Linear Least Squares SDOF Algorithm for Identifying Eigenvalues and Residues,* Proceedings of the 21st International Modal Analysis Conference, Orlando, FL, 2003.

[4] **Ginsberg, J. H., Zaki, B. R., Drexel, M. V.**, *Application of the Mode Isolation Algorithm to the Identification of a Complex Structure,* Proceedings of the 20th International Modal Analysis Conference, Los Angeles, CA, 2002.

[5] **A. Leissa**, *Vibration of Plates*, ASA Press, Melville, New York, 1993 reprint.

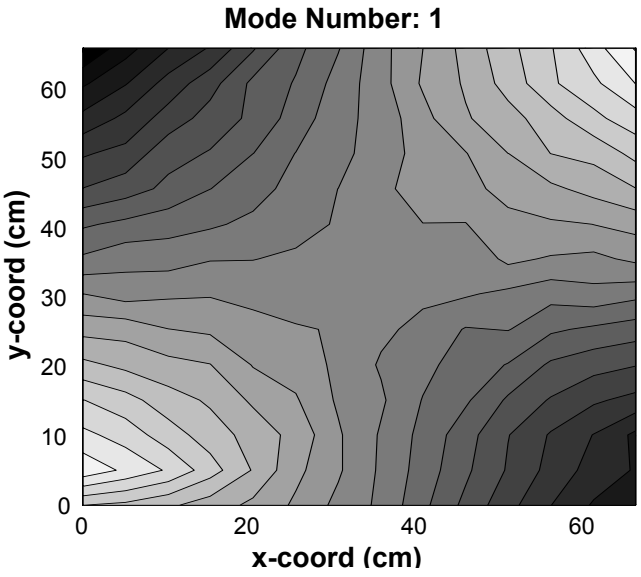

Figure 4: Contour plot of first mode-LLS-SDOF.

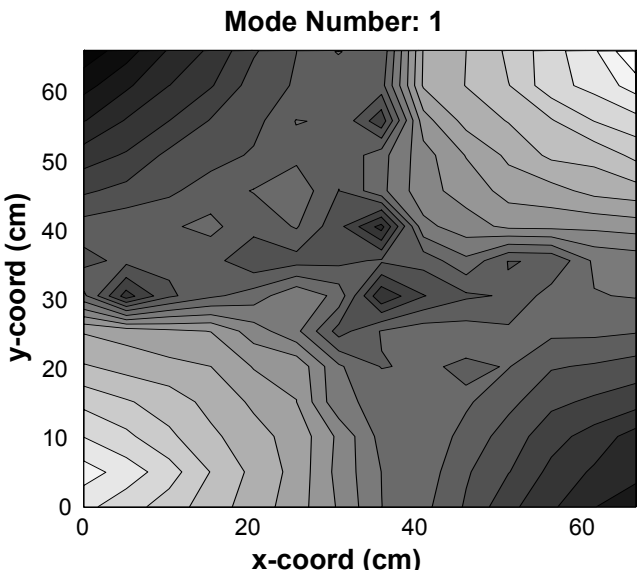

Figure 5: Contour plot of first mode-STAR.

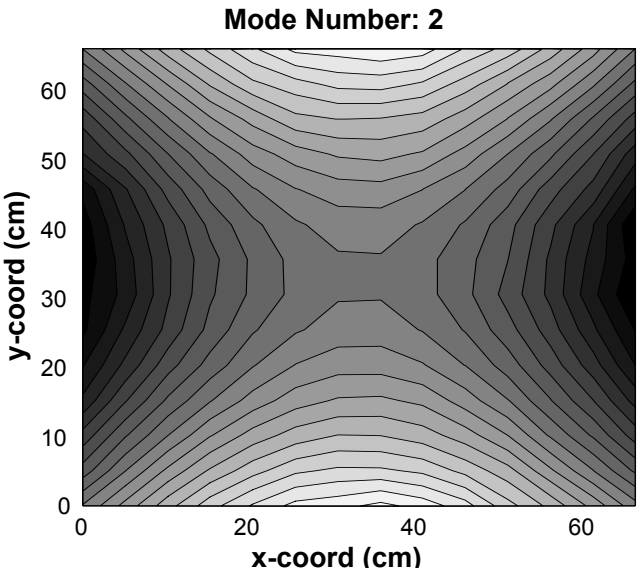

Figure 6: Contour plot of second mode-LLS-SDOF.

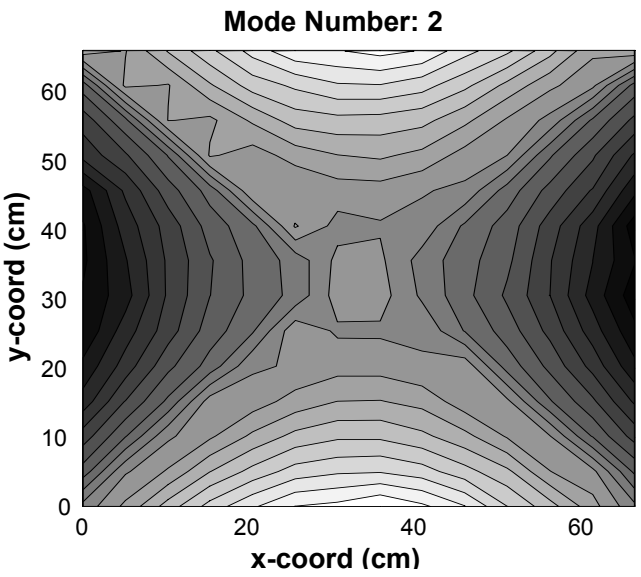

Figure 7: Contour plot of second mode-STAR.

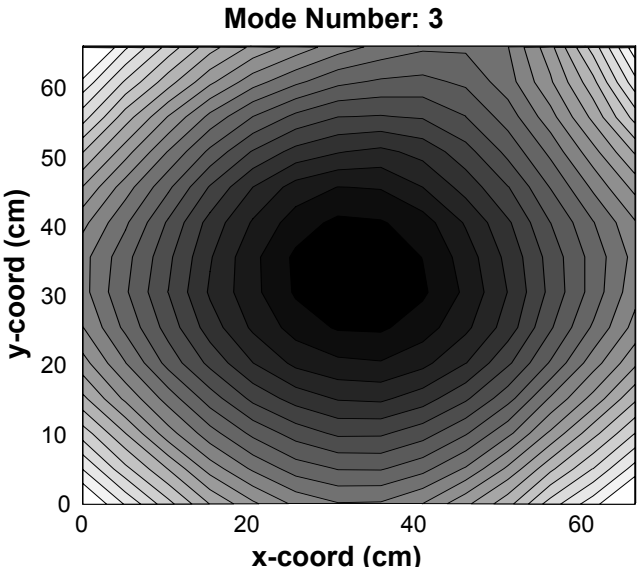

Figure 8: Contour plot of third mode-LLS-SDOF.

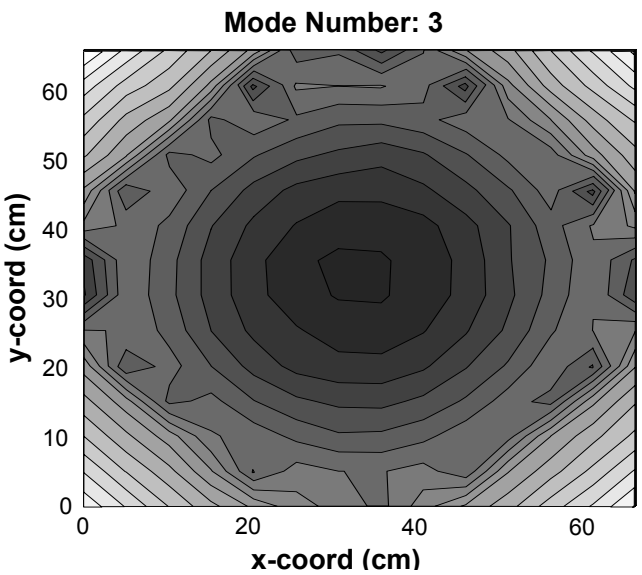

Figure 9: Contour plot of third mode-STAR.

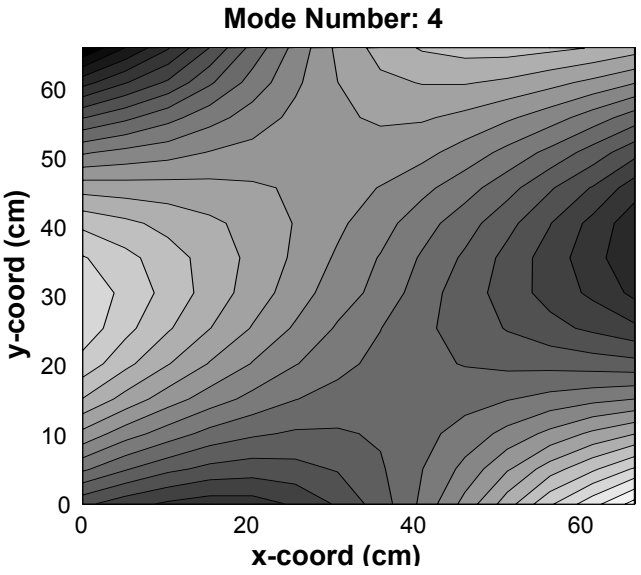

Figure 10: Contour plot of fourth mode-LLS-SDOF.

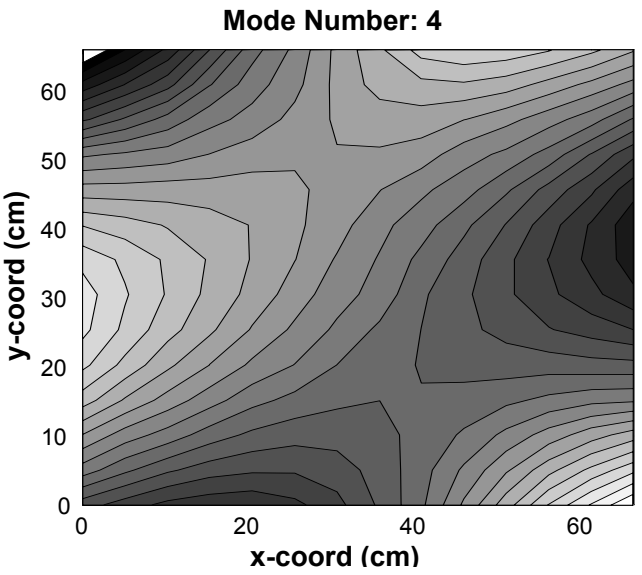

Figure 11: Contour plot of fourth mode-STAR.